Transactions of the Korean Nuclear Society Autumn Meeting
Gyeongju, Korea, October 29-30, 2026

AI-assisted Inverse Analysis of Fabrication-Dependent Creep Parameters for ATF Cr Coatings using MERCURY

Ganghyeon Bae, Hwasung Yeom*
Division of Advanced Nuclear Engineering, Pohang University of Science and Technology (POSTECH)
**Corresponding author: hyeom@postech.ac.kr*

Keywords : MERCURY, Creep parameters, Cr coatings, AI, Surrogate modeling

1. Introduction

Cr-coated Zr alloy cladding designs have been widely investigated as a promising accident tolerant fuel (ATF) cladding concept. Various fabrication methods have been employed to fabricate Cr coatings, including cold spray (CS) and physical vapor deposition (PVD) techniques. These fabrication methods can result in distinct coating microstructures, residual stress states, and mechanical properties, potentially leading to different high-temperature creep responses. Consequently, a single set of creep parameters should not adequately represent Cr coatings produced by different fabrication methods.

Direct experimental characterization of the creep behavior of micrometer-scale Cr coatings remains challenging. Due to the limited availability of creep data for Cr coatings, creep parameters of bulk Cr have been used in Cr-coated cladding ballooning and burst analyses [1-2]. Therefore, an inverse analysis approach using ballooning and burst test data with fuel performance codes was reported for determining the creep parameters for a specific Cr coating design [3].

In this study, fabrication-dependent creep parameters were estimated through inverse analysis using ballooning and burst test data for four different Cr-coated Zr alloy cladding conditions, including helium cold spray (HCS), nitrogen cold spray (NCS), magnetron sputtering (MS), and HiPIMS. An automated inverse-analysis framework was developed by coupling the fuel performance code MERCURY (Multi-dimensional Entire fuel Rod Code for Understanding Reaction Yield Behaviors) V1.0 developed by Korea Atomic Research Institute (KAERI) with an artificial intelligence (AI) agent that performs input generation, simulation execution, and output processing. Surrogate models were further incorporated to reduce the computational cost of the inverse analysis and accelerate parameter identification.

2. Methods and Results

The ballooning and burst experimental data for uncoated Optimized ZIRLO^{TM} (OPZ) and Cr-coated Zr alloy cladding fabricated by HCS, NCS, MS and HiPIMS were obtained from previous studies [3-5]. These datasets include the test conditions and measured burst behaviors required for the inverse analysis.

2.1 AI-assisted Inverse Analysis Framework

An AI-assisted inverse analysis framework was developed to identify fabrication-dependent creep parameters for Cr coatings. In MERCURY, the Cr coating and Zr alloy substrate were modeled separately with a multi-layer approach. The creep parameters of the Zr alloy substrate were first identified using the uncoated OPZ cladding data, followed by the identification of fabrication-dependent creep parameters for the Cr coatings.

The high-temperature creep behavior was modeled with the Norton creep equation implemented in MERCURY. The creep parameters to be identified were the creep coefficient (A), stress exponent (n), and activation energy (Q), which govern the magnitude of the creep strain rate and its dependence on stress and temperature.

$$\dot{\varepsilon} = A\sigma^n exp\left(-\frac{Q}{RT}\right)$$

Axisymmetric finite element models were constructed based on the geometry of each experimental specimen. The cladding length and substrate and Cr coating thickness were specified individually for each test case. The mesh consisted of 50 elements along the axial direction, 4 elements through the substrate thickness, and 1 element through the Cr coating thickness. The temperature and internal pressure histories were applied as time-dependent boundary conditions. Candidate creep parameter sets were generated using optimal Latin hypercube sampling (OLHS) to explore the prescribed parameter space.

For each creep parameter set sampled through OLHS, the Codex AI agent automatically generated a MERCURY input file, executed the simulation, and processed the output to evaluate the crossing-time error. The crossing time was defined as the time at which the simulated hoop strain reached the experimentally measured burst strain. The difference between this crossing time and the experimental burst time was used as the crossing-time error. The optimal creep parameter set was selected as the parameter set with the minimum absolute crossing-time error among the simulated cases.

2.2 Surrogate-assisted Parameter Search

The radial basis function (RBF) surrogate model was constructed using MERCURY simulation results

obtained from parameter sets selected by OLHS. For OPZ, 15 cases were used for training and 15 additional cases were used for testing. The creep parameters were used as the input variables, and the crossing time error was used as the surrogate model output. A thin-plate spline kernel was employed as the RBF. As shown in Fig. 1, the surrogate predictions for the validation dataset closely followed the parity line, with an R^2 of 0.99 and an RMSE of 1.50%.

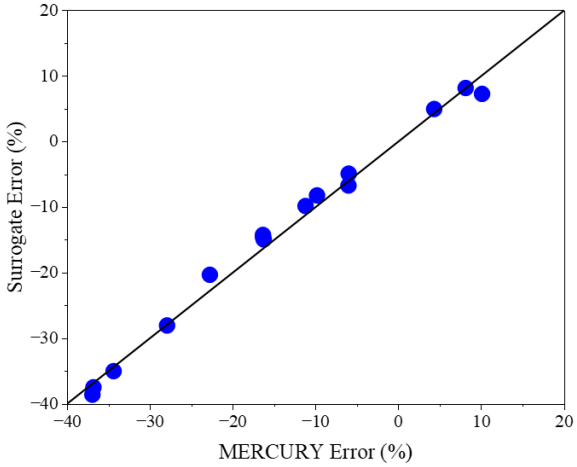


Fig. 1. Parity plot of crossing-time errors predicted by the RBF surrogate model and calculated by MERCURY for the OPZ validation dataset.

The constructed surrogate models were used to evaluate a large number of candidate parameter sets within the prescribed parameter space. The top five candidates with the lowest absolute surrogate-predicted crossing-time errors were subsequently evaluated using MERCURY. As summarized in Table I, the fourth-ranked candidate showed the smallest crossing-time error in the direct MERCURY simulations, with an error of 0.12%.

Table I. Surrogate-selected creep parameter sets for OPZ and the best OLHS sample with MERCURY crossing-time errors.

Rank	A [$MPa^{-n}s^{-1}$]	n [-]	Q [J/mol]	Surrogate error [%]	MERCURY error [%]
1	7877	5.41	3.03E+05	-0.0004	+1.48
2	9460	5.89	3.19E+05	+0.0012	-0.58
3	8824	5.68	3.13E+05	-0.0020	+1.74
4	**9037**	**6.27**	**3.31E+05**	**-0.0025**	**-0.12**
5	8745	5.96	3.21E+05	-0.0031	+0.32
Best OLHS	8667	5.82	3.16E+05		+0.12

2.3 Evaluation of Fabrication-Dependent Creep Parameters

The identified creep parameters were evaluated by comparing the simulated hoop strain histories with those predicted using bulk Cr creep parameters. As shown in Fig. 2, the simulations with the inverse analysis results showed improved agreement with the experimentally measured burst points. These results suggest that incorporating fabrication-dependent creep parameters can improve the accuracy of burst behavior predictions for Cr-coated cladding compared with the use of bulk Cr creep properties.

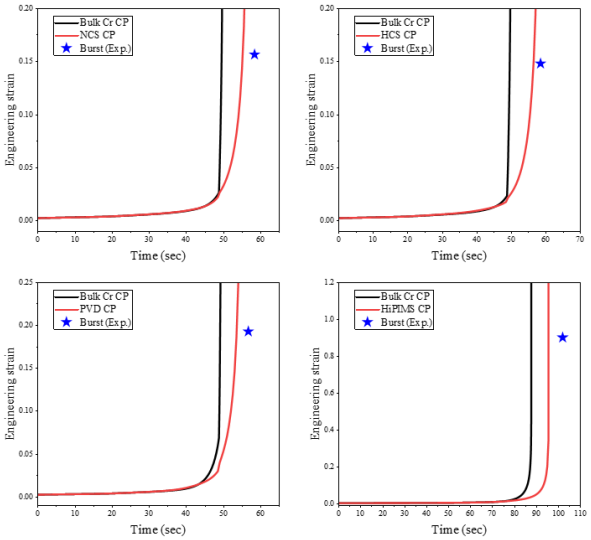


Fig. 2. Comparison of simulated hoop strain histories using bulk Cr and inverse analysis fabrication-dependent creep parameters with experimental burst conditions.

3. Conclusions

An AI-assisted inverse analysis framework was developed to identify fabrication-dependent creep parameters for Cr coatings using ballooning and burst test data. The framework combined the MERCURY fuel performance code with automated input generation, simulation execution, and output processing, while a surrogate model was used to efficiently explore the creep parameter space.

The identified creep parameters provided better agreement with the measured burst conditions than using bulk Cr creep parameters. These results suggest that considering fabrication-dependent creep parameters may improve the deformation of Cr-coated cladding under ballooning and burst conditions.

ACKNOWLEDGEMENTS

This work was supported by the Korea Institute of Energy Technology Evaluation and Planning (KETEP) and the Ministry of Climate, Energy & Environment (MCEE) of the Republic of Korea (No. RS-2026-25533036).

REFERENCES

[1] M. Wagih, B. Spencer, J. Hales, and K. Shirvan, Fuel performance of chromium-coated zirconium alloy and silicon carbide accident tolerant fuel claddings, Annals of Nuclear Energy, Vol. 120, pp. 304–318, 2018.
[2] Z. Ma, K. Shirvan, Y. Wu, and G. H. Su, Numerical investigation of ballooning and burst for chromium coated Zircaloy cladding, Nuclear Engineering and Design, Vol. 383, p. 111420, 2021.
[3] S. U. Lee, H. Kim, M. Ševeček, and M. Király, High-temperature creep behavior of Cr-coated Optimized ZIRLO™ cladding via inverse analysis based on finite element method, Nuclear Engineering and Design, Vol. 444, p. 114383, 2025.
[4] I. Alakiozidis, M. L. N. de Sousa, A. Gauthier, C. Hunt, M. Maric, A. Ambard, Z. Shah, and P. Frankel, Semi-integral LOCA testing of Cr-coated Optimized ZIRLO™, Journal of Nuclear Materials, Vol. 610, p. 155766, 2025.
[5] M. Ridley, S. Bell, B. Garrison, T. Graening, N. Capps, Y. F. Su, P. Mouche, B. Johnston, and K. Kane, Effects of Cr/Zircaloy-4 coating qualities for enhanced accident tolerant fuel cladding, Annals of Nuclear Energy, Vol. 188, p. 109799, 2023.